RM No. A7G17

Copy 2

NACA

5 DEC 1947

RESEARCH MEMORANDUM

COMPARISON BETWEEN FLIGHT-MEASURED AND CALCULATED SPAN LOAD DISTRIBUTION AT HIGH MACH NUMBERS

By L. Stewart Rolls

Ames Aeronautical Laboratory
Moffett Field, Calif.

NATIONAL ADVISORY COMMITTEE
FOR AERONAUTICS

WASHINGTON
November 26, 1947

NACA RM No. A7G17

NATIONAL ADVISORY COMMITTEE FOR AERONAUTICS

RESEARCH MEMORANDUM

COMPARISON BETWEEN FLIGHT-MEASURED AND CALCULATED SPAN LOAD DISTRIBUTION AT HIGH MACH NUMBERS

By L. Stewart Rolls

SUMMARY

The spanwise loading has been computed, by two different methods, on the wing of an airplane for which pressure-distribution measurements were available from flight tests up to a Mach number of 0.866. One set of the calculations was based on a generalized method of the lifting-line theory utilizing high-speed wind-tunnel data, while the other set employs an approximate semielliptical distribution. The comparison between the measured and calculated distributions has been made on the basis of equal wing-panel normal-force coefficients.

To obtain a valid comparison it was necessary to consider the upfloat of the aileron which occurred at the higher Mach numbers. A fairly close agreement was obtained by both methods for these conditions, especially at the highest values of C_N considered. It was shown that, up to 0.866 Mach number, neglect of aileron upfloat in span load calculations might produce a more serious shift in the span load distribution than would occur from nonconsideration of the compressibility effects on the section lift-curve slope and angle of zero lift.

INTRODUCTION

A great deal of consideration has been given to the accuracy of computed span load distribution at high speeds due to the change in the distribution occurring at high Mach numbers. Recently, measurements of the wing pressure distributions have been made on a jet-propelled airplane in flight up to a Mach number of 0.866 (reference 1). These data have given an opportunity for checking the accuracy of methods of computing high-speed span load distribution. This report presents comparisons between measured span load and span load as computed by two methods.

In the first case the comparison was made between measured span load distributions and calculated values, using the method of reference 2, a generalized method by which the effects of compressibility and abrupt twist are treated by a process of successive approximations utilizing section data. The high-speed section data necessary for this method of calculating span load distribution was obtained from the results of tests in the Ames 1- by 3-1/2-foot high-speed wind tunnel.

The second comparison was made between the measured distributions and the calculated distributions based on the method of reference 3 which assumes an approximate semielliptical distribution of lift.

SYMBOLS

A_Z airplane normal-acceleration factor (Z/W)

b wing span, feet

c wing section chord, feet

c_{l_a} section additional lift coefficient

c_n section normal-force coefficient,

$$\left[\int_0^c (P_L - P_U) \, d\left(\frac{x}{c}\right) \right]$$

C'_{BM} wing-panel bending-moment coefficient,

$$\left[\frac{b}{2S} \int_0^{b/2} c_{nc} \left(\frac{y}{b/2} - 0.25\right) \, d\left(\frac{y}{b/2}\right) \right]$$

C'_N wing-panel normal-force coefficient,

$$\left[\frac{b}{2S} \int_0^{b/2} c_{nc} \, d\left(\frac{y}{b/2}\right) \right]$$

C_N	airplane normal-force coefficient (WA_Z/qS)
M	Mach number
P_L	pressure coefficient on lower surface of wing
P_U	pressure coefficient on upper surface of wing
q	dynamic pressure, pounds per square foot
S	wing area, square feet
x	chordwise location from leading edge, feet
y	spanwise location from plane of symmetry, feet
W	airplane gross weight, pounds
Z	aerodynamic normal force on airplane, pounds
δ_a	aileron control-surface deflection (positive trailing edge down), degrees
α	angle of attack of airfoil section, degrees
α_a	angle of attack of airplane thrust axis, degrees

DESCRIPTION OF AIRPLANE AND INSTRUMENTATION

The airplane used in these flight tests was a turbo-jet-propelled fighter. Figures 1 and 2 are photographs of the airplane as instrumented for flight. A three-view drawing showing the spanwise locations of wing pressure orifices is presented in figure 3. The basic dimensions of the airplane are presented in table I. The geometric twist of the wing is shown in figure 4.

Standard NACA photographically recording instruments were used to record the wing orifice pressures and other quantities during flight. A more complete description of the instrumentation and accuracy of the experimental data may be found in reference 1.

RESULTS AND DISCUSSION

The primary comparison made in this report is between the measured

distribution and the calculated distribution obtained using the method of reference 2. These calculations are based on a generalized method of applying lifting-line theory, using a series of successive approximations; that is, from the fundamental downwash equations, a spanwise distribution of downwash angle is found for some initial assumed loading and, from the difference between the geometric and computed downwash angles at each station of the span, the effective angles of attack are determined. When the effective angles of attack are applied to each section lift curve, lift coefficients at each station are obtained which, when multiplied by the ratio of the chord at the station to the mean chord, define a new check distribution. As a second approximation, an assumed span loading is taken between the first approximation and the check points. The process is continued until the check loading coincides with that from which it was derived.

To enable the comparison to be made on the basis of equal wing-panel normal-force coefficients, it was necessary to compute the wing-panel normal-force coefficient variation with airplane angle of attack. These calculations were made by the method of reference 2, using the two-dimensional section data obtained on the NACA 65_1-213(a=0.5) airfoil in the Ames 1- by 3-1/2-foot high-speed wind tunnel. (See fig. 5.) The calculated variation of wing-panel normal-force coefficient with airplane angle of attack are presented in figure 6.

The results presented in figure 7 show the comparison between measured and calculated span load distribution for several values of Mach number and airplane normal-force coefficients. In comparing the chordwise loading $c_n c$ at each individual spanwise station, considerable variation between the calculated and measured loading will be noted at Mach numbers above 0.60.

An earlier report (reference 1) on this same installation attributed a portion of the inboard shift in the spanwise load distribution measured in flight to the upfloating aileron which occurred in flight at the higher Mach numbers. For the calculated distribution shown in figure 7, no consideration was made for the effect of an upfloating aileron. Extrapolating the section data shown in figure 5, for M = 0.84, to the aileron angles taken from reference 1 (shown in fig. 8) the span load distribution presented in figure 9 was computed and compared with flight results.

Further comparison of the sectional loading was obtained by computing the wing-panel bending-moment coefficient based on the bending moment about the 25-percent semispan station. To enable

the comparison to be based on the same wing area, it was necessary to extend the measured data inboard from wing station 65 (27.8 percent semispan) to the center line of the fuselage. The errors involved in this extrapolation are thought to be small. Figure 10 compares the bending-moment coefficients for the measured and calculated distribution as a function of Mach number and airplane normal-force coefficients. This comparison indicates that the center of pressure for the calculated distributions at values of C_N of 0.2 and 0.6 is farther outboard than the center of pressure for the measured distribution. By considering the effect of aileron deflection, points spotted on figure 10 at $M = 0.84$, better agreement is shown. The best correlation was obtained for an airplane normal-force coefficient of 0.60 at which time the aileron was floating 4° up. At the lower values of normal-force coefficient the effect of the upfloating aileron is not as noticeable. One explanation for this difference at the lower values of C_N is the possibility that the results from the small-scale model of the 1- by 3-1/2-foot high-speed wind-tunnel test indicated a lower value of control-surface effectiveness at the low lift coefficients than at the higher values.

To determine the necessity for using the method based on high-speed-tunnel data and to check the validity of using a low-speed method, the distribution was calculated using the usual method of reference 3. This method is based on two assumptions. First, the additional loading coefficient $c_{l_a}c/C_N$ is a mean between the wing chord and a semiellipse having the same area as the wing, and, second, the basic lift distribution is a mean between the spanwise camber lift line and the geometric lift-coefficient distribution due to angle of twist. The total distribution is the sum of the additional lift and basic lift distribution. In this method the aileron is treated as a case of an abrupt twist. No corrections are made for the effects of compressibility.

In figure 11, a comparison is made between the results of the calculations performed using the two different methods. These comparisons indicate a fairly close correlation in all cases where the calculations were made with an aileron angle of 0°. However, for the case shown in figure 11(c), where the calculations were corrected for an aileron deflection of 4° up, the bending moment calculated by the method of reference 3 is about 20 percent lower than the bending moment derived from reference 2.

The data and calculations in this report indicate that, for the airplane under consideration, the effect of aileron deflection is more critical from the standpoint of spanwise distribution than the effect of compressibility on section lift-curve slope and angle

of zero lift. In this particular case with the aileron deflected up, there is an inboard shift in the load thus causing a decrease in the bending moment; and it is apparent that neglect of the effect of aileron upfloat in design calculations of loading would be conservative. It is conceivable, however, that in some cases wing and aileron characteristics might be such as to cause a downward deflection of the aileron at high Mach numbers, thus producing greater bending moments. It is recommended, therefore, that calculations of spanwise loading at the higher Mach numbers include consideration of the effect of aileron deflection. In this regard it is apparent that research is necessary to provide methods for estimating aileron deflections at higher Mach numbers.

CONCLUDING REMARKS

Over the Mach number range for which tests were made, it was shown in this particular case that considerable variation occurred between the section normal-force coefficient c_n as measured and as calculated where no deflection was considered. This demonstrated the necessity of considering the aileron angle at high Mach numbers to obtain a correlation between measured and calculated distributions. In this case better correlation was obtained between measured and calculated values of span load distribution at higher airplane normal-force coefficients than at lower airplane normal-force coefficients. Comparison of measured and calculated values of span load distribution showed that the upfloating aileron had a greater effect on the span load distribution than changes in lift-curve slope and angle of zero lift due to compressibility. It is recommended that calculations of spanwise loading at high Mach numbers include the effect of aileron deflections.

The difference between the calculated distributions, using either reference 2 or 3, and the measured distribution indicated by these results are within the accuracy of the preliminary design considerations. Hence, in this particular case the simple method (reference 3) gave as good an agreement with test results as reference 2 but involved approximately one-third the time and did not require additional tests to obtain airfoil-section data.

Ames Aeronautical Laboratory,
National Advisory Committee for Aeronautics,
Moffett Field, Calif.

REFERENCES

1. Brown, Harvey H. and Clousing, Lawrence A.: Wing Pressure-Distribution Measurements Up to 0.866 Mach Number in Flight on a Jet-Propelled Airplane. NACA TN No. 1181, 1947.

2. Boshar, John: The Determination of Span Load Distribution at High Speeds by Use of High-Speed Wind-Tunnel Section Data. NACA ACR No. 4B22, 1944.

3. Flatt, J.: Evaluation of Methods for Determining Spanwise Lift Distribution. Army Air Forces Tech. Rep. No. 4952, June 1943.

TABLE I.- BASIC DIMENSIONAL DATA OF TEST AIRPLANE

Wing	
Area, square feet	237
Span, feet	38.9
Root chord, feet	9.167
Tip chord, feet	3.333
Aspect ratio	6.4
Taper ratio	0.363
Mean aerodynamic chord, feet	6.72
Dihedral of trailing edge, degrees	3.83
Incidence, root chord, degrees	1
Incidence, tip chord, degrees	-0.50
Root section	65_1-213, a=0.50
Tip section	65_1-213, a=0.50
Percent line straight	52.0
Aileron	
Area aft of hinge line (one side), square feet	8.57
Span, feet (one side)	7.21
Mean aerodynamic chord, feet	1.216
Hinge-line location, percent chord	75.0
Tabs	Trim tab on left aileron

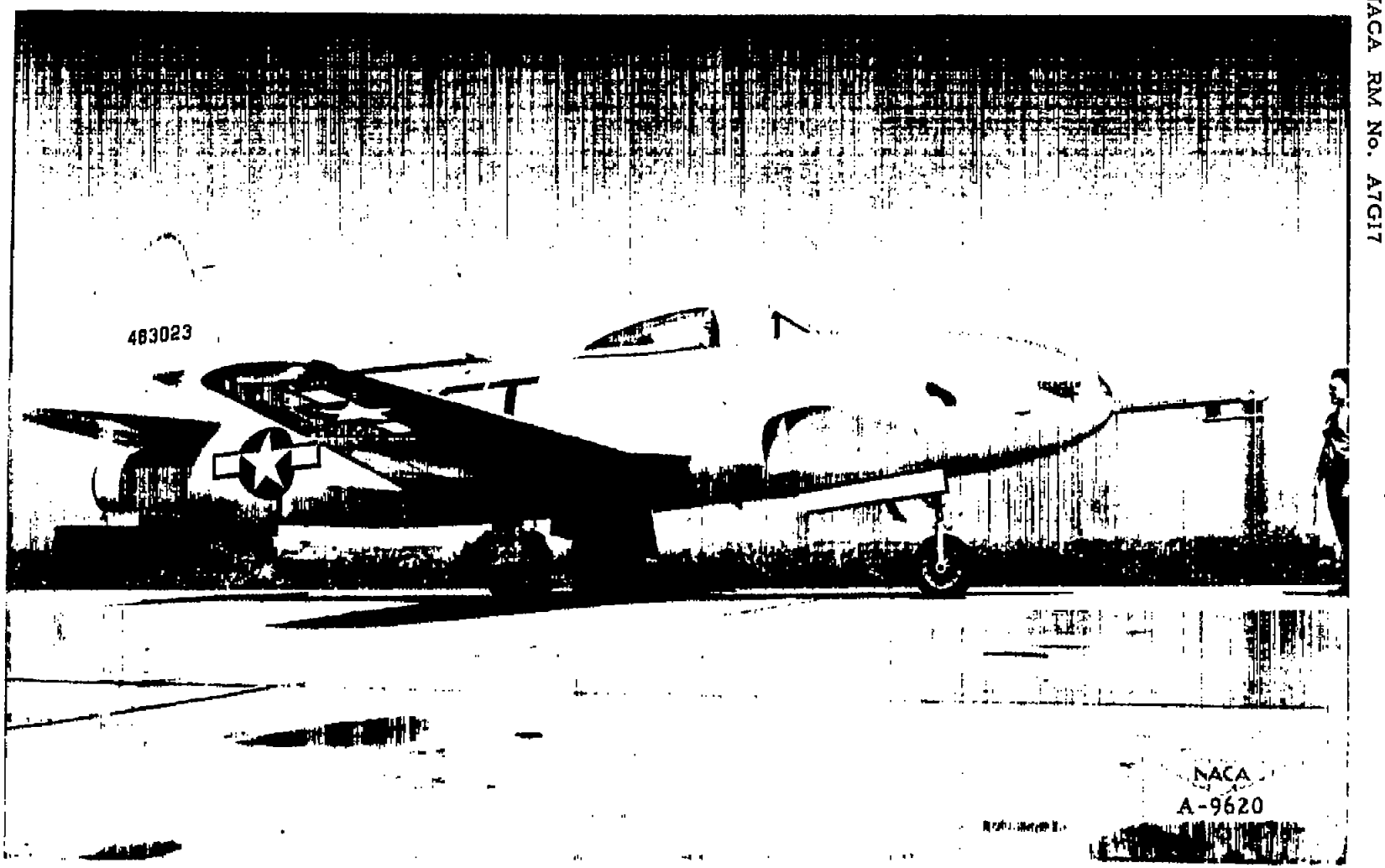

Figure 1.- Three-quarter side view of the test airplane.

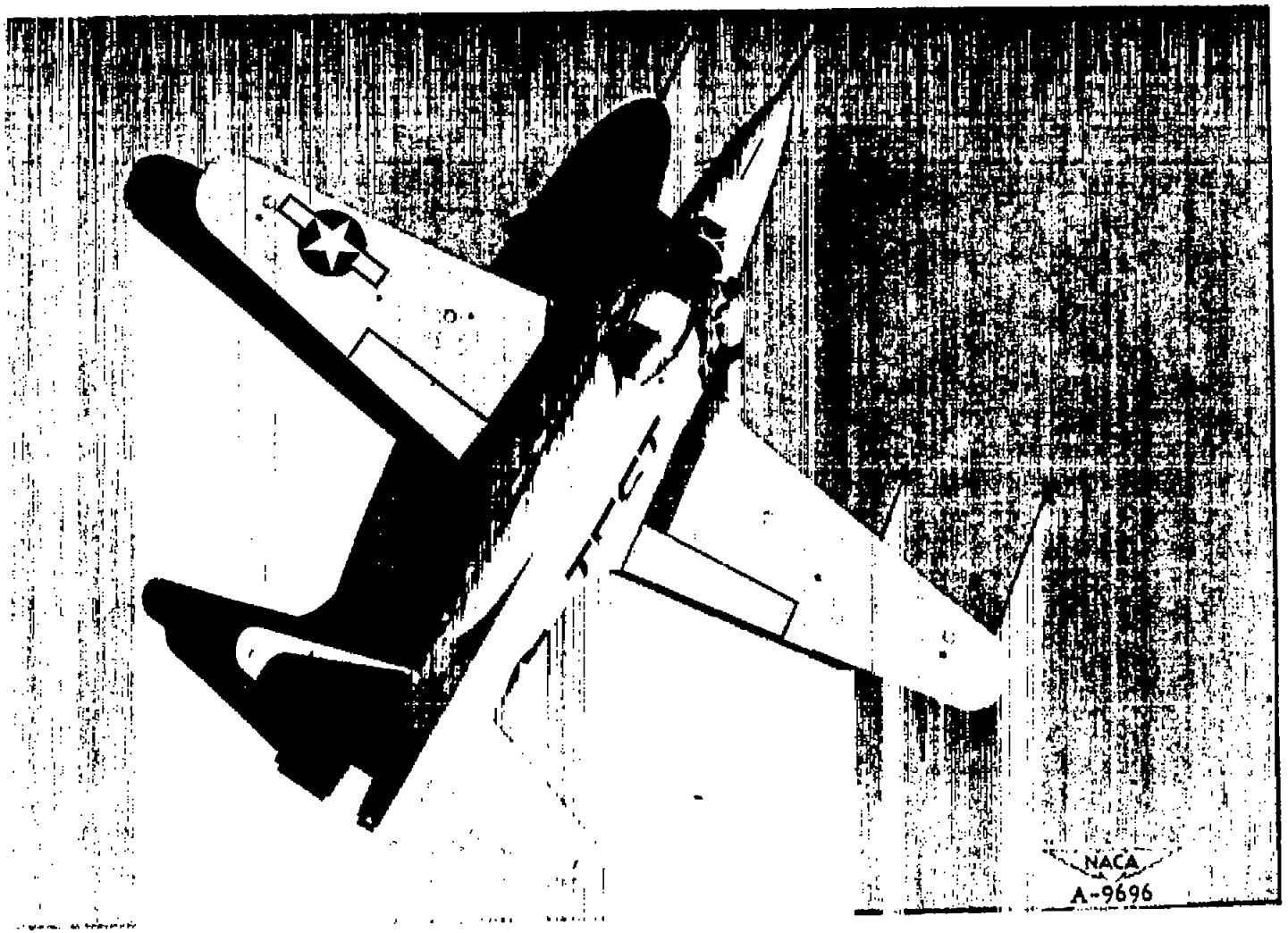

Figure 2.- Plan view of the test airplane.

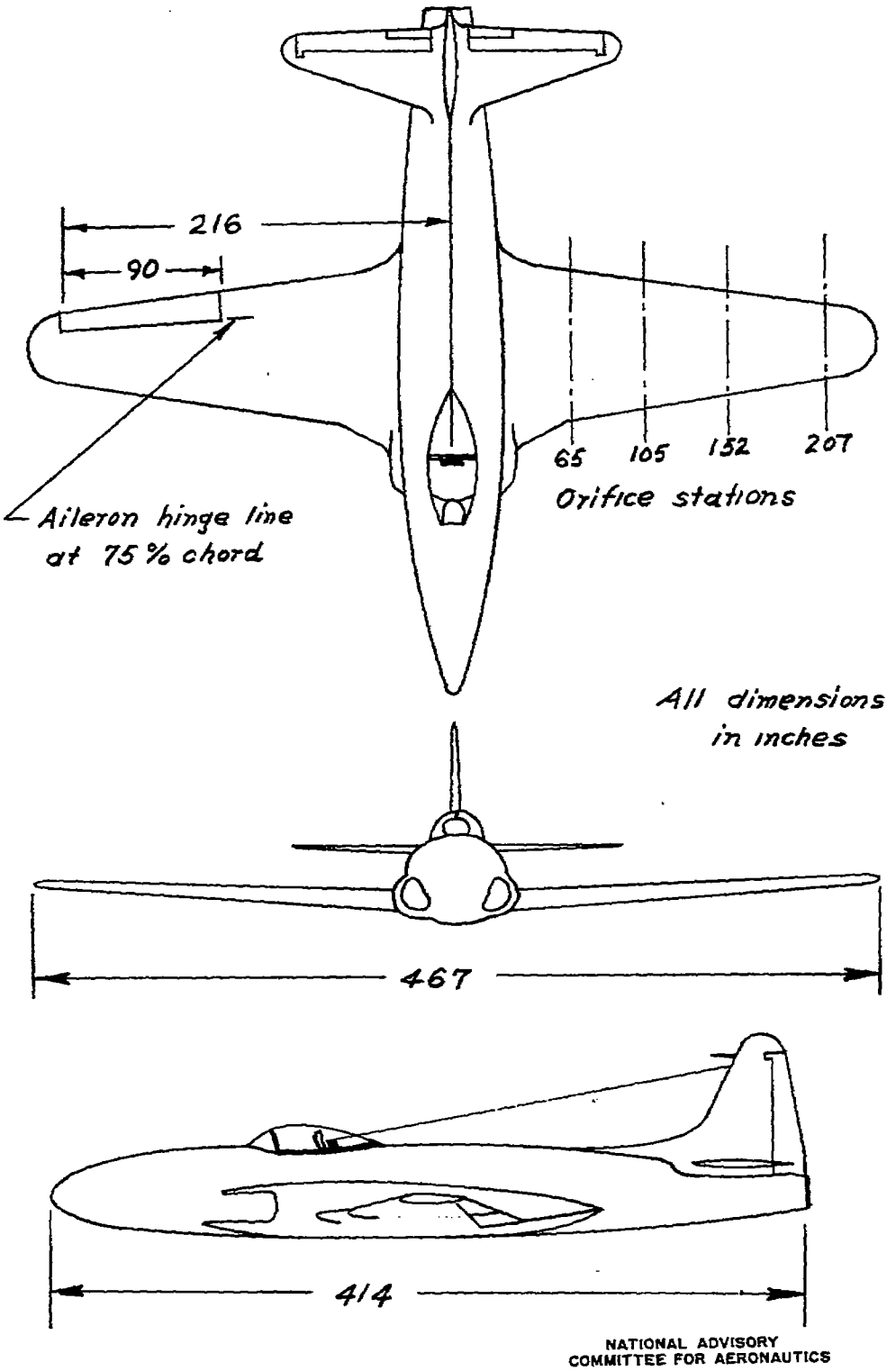

Figure 3.- Three-view drawing of the test airplane.

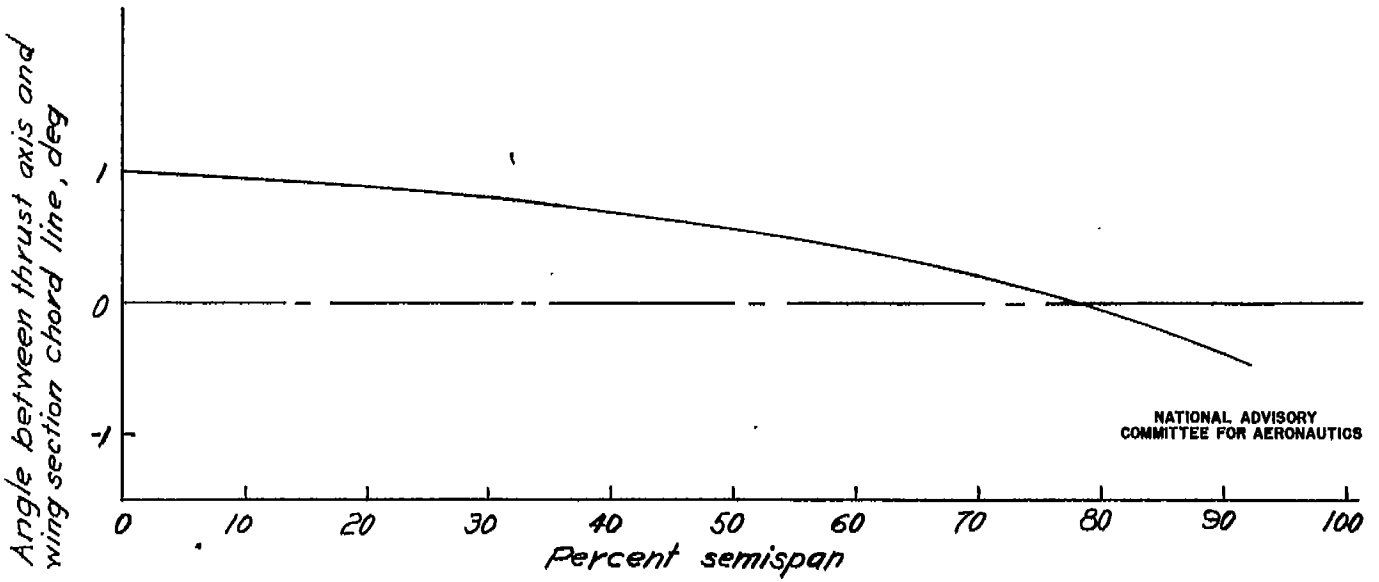

Figure 4.— Geometric twist in the wing of the test airplane.

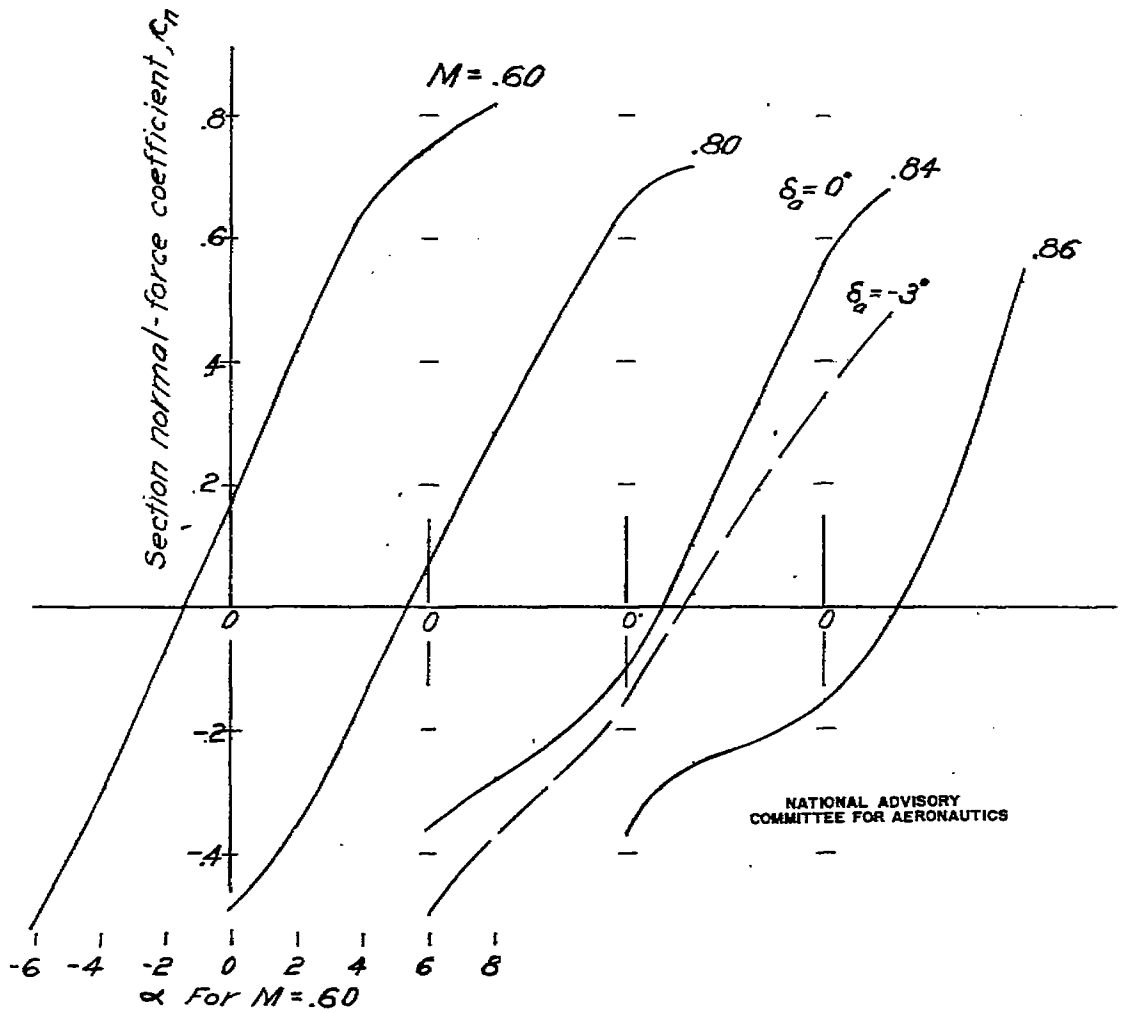

Figure 5.— Section data on the NACA 65_1-213 (a = .5) airfoil from tests in the Ames 1 x 3½ foot High-Speed Wind Tunnel.

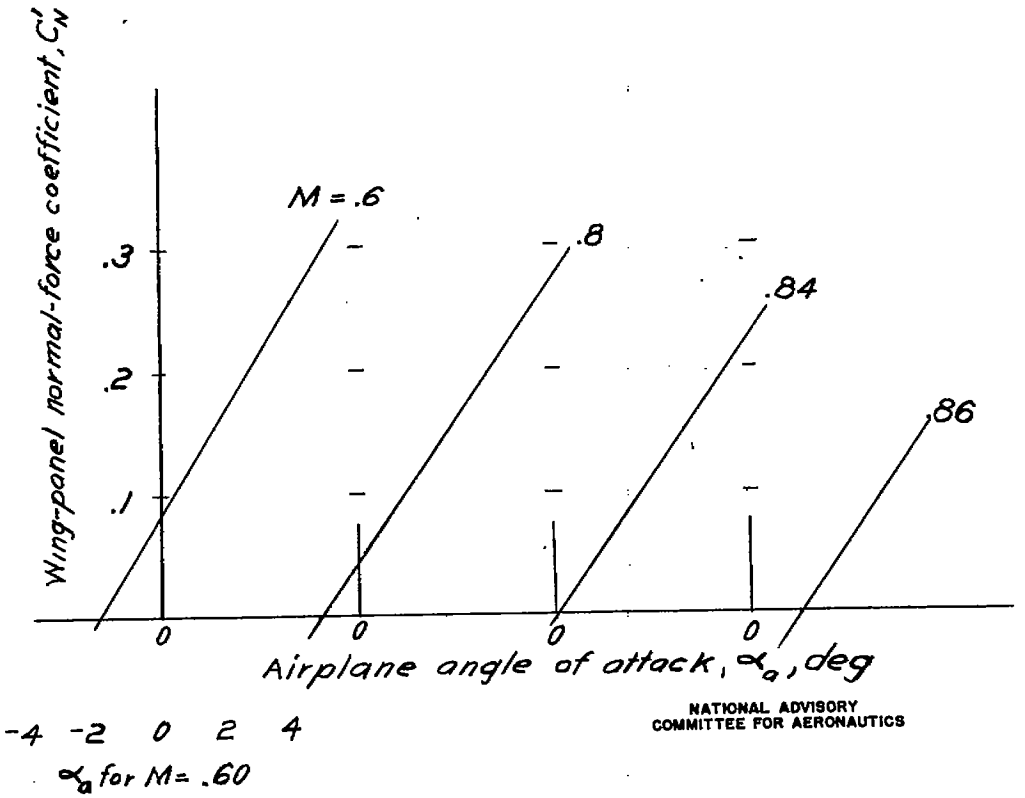

Figure 6.— Calculated variation of wing-panel normal-force coefficient with airplane angle of attack.

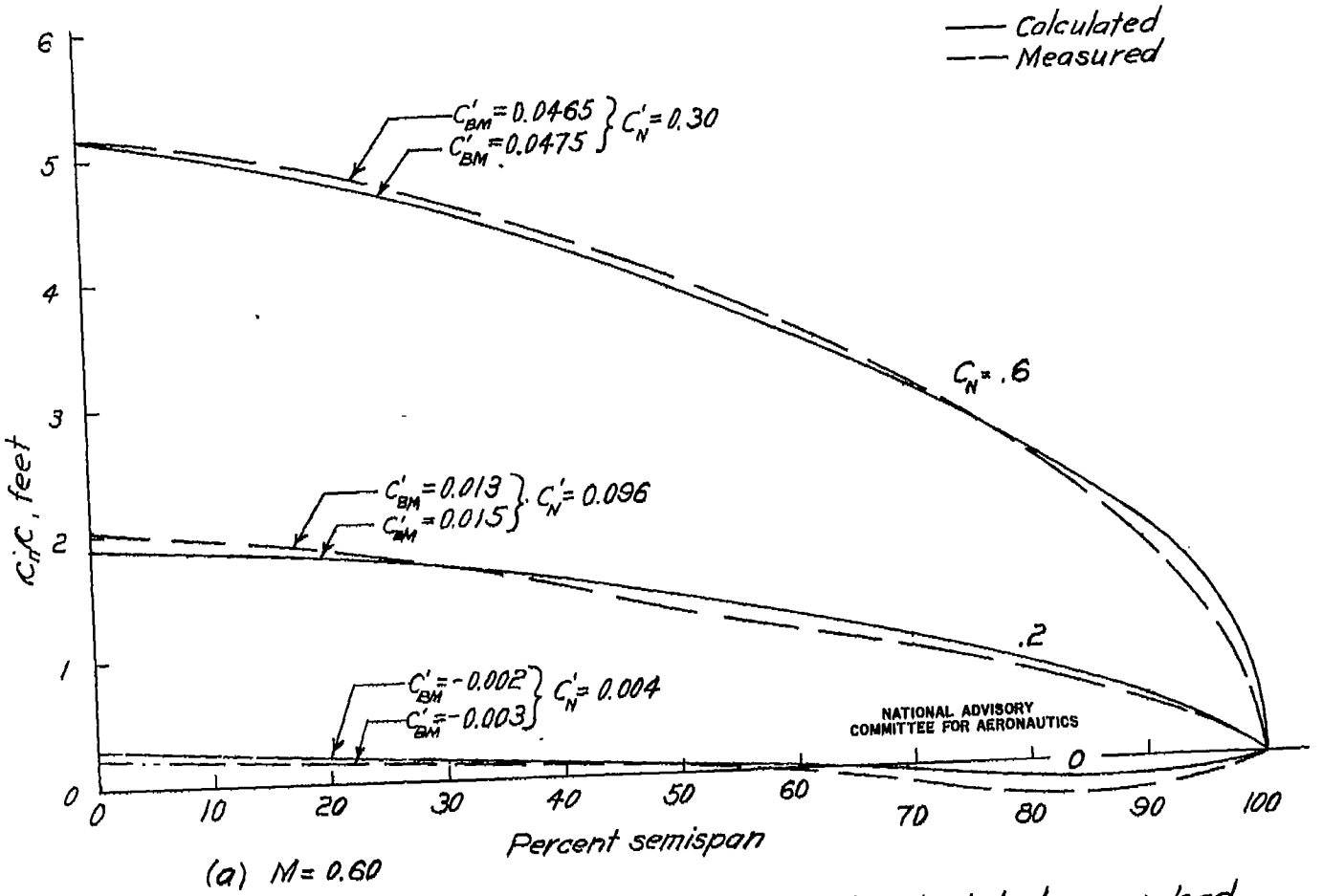

(a) M = 0.60

Figure 7.— Comparison between measured and calculated span load distribution using method of reference 2. Aileron undeflected.

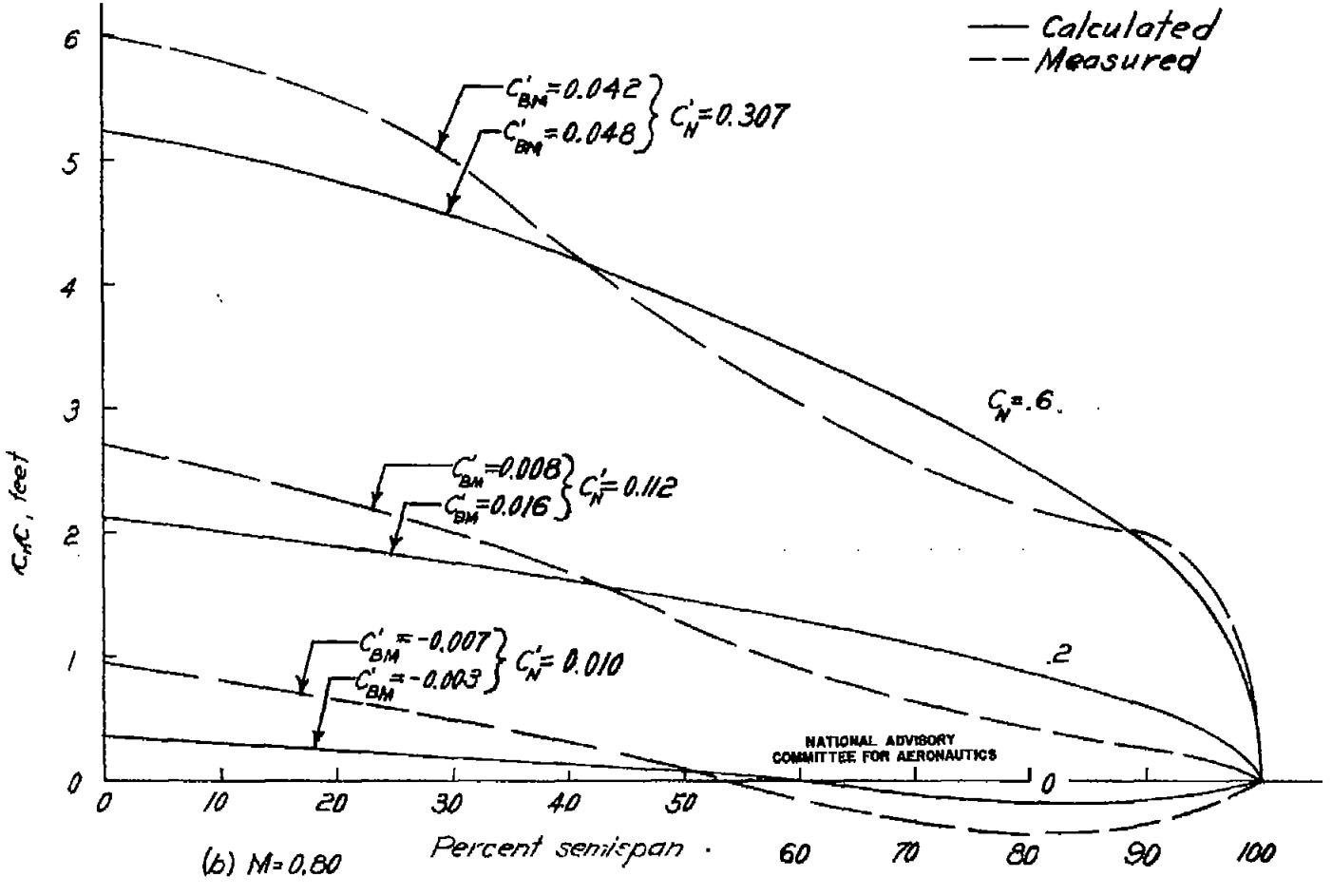

(b) M=0.80

Figure 7.— Continued.

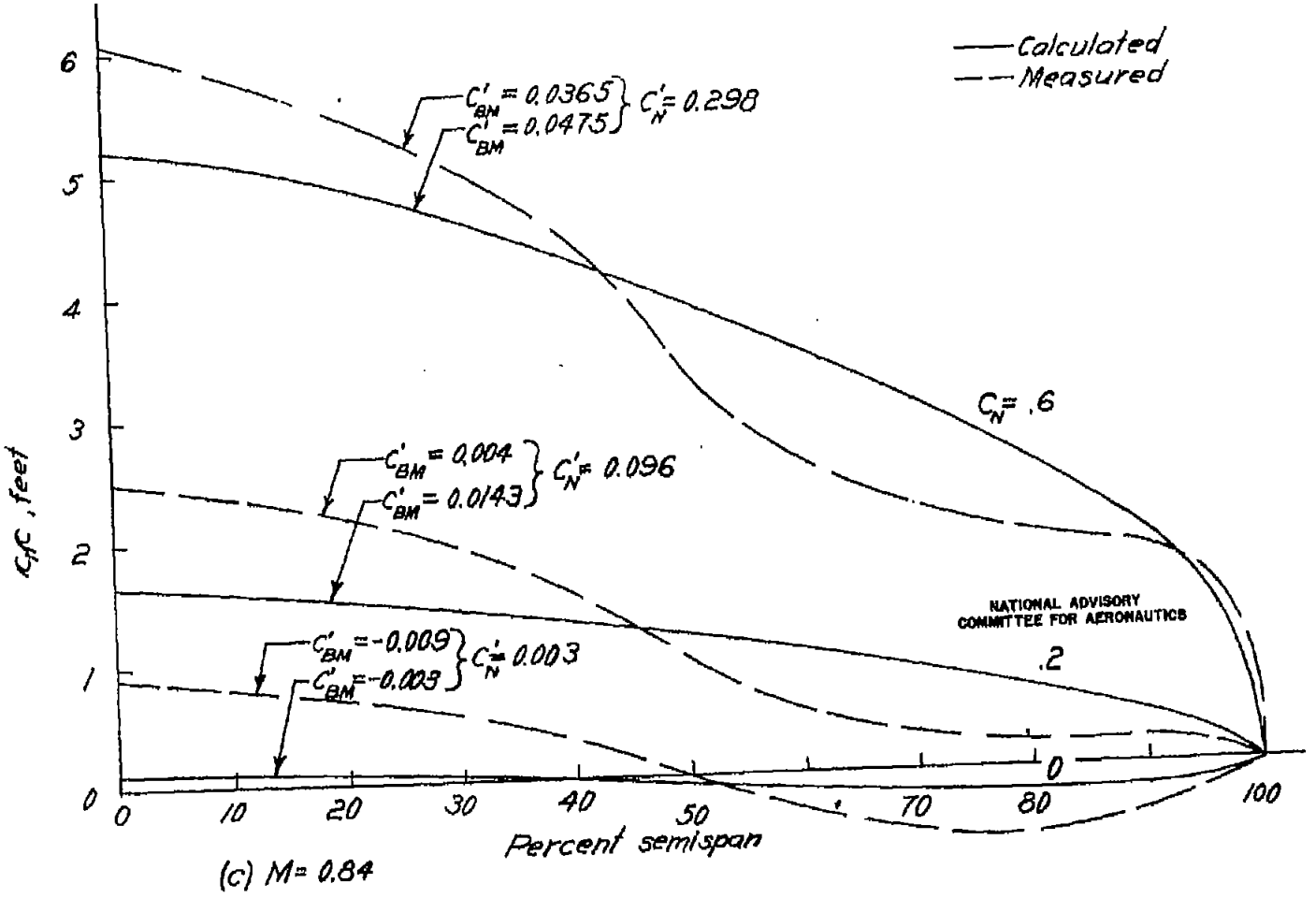

(c) M= 0.84

Figure 7.—Continued.

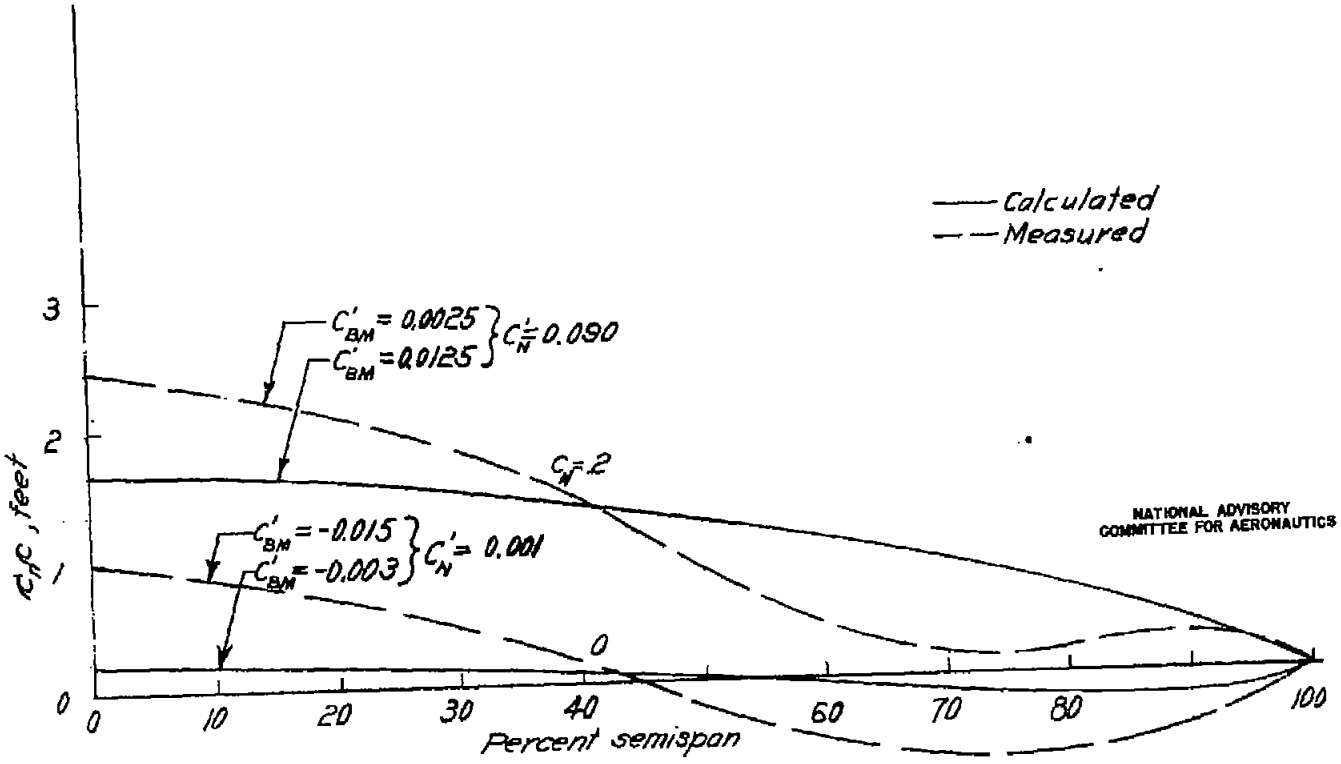

(d) $M = 0.86$

Figure 7.—Concluded.

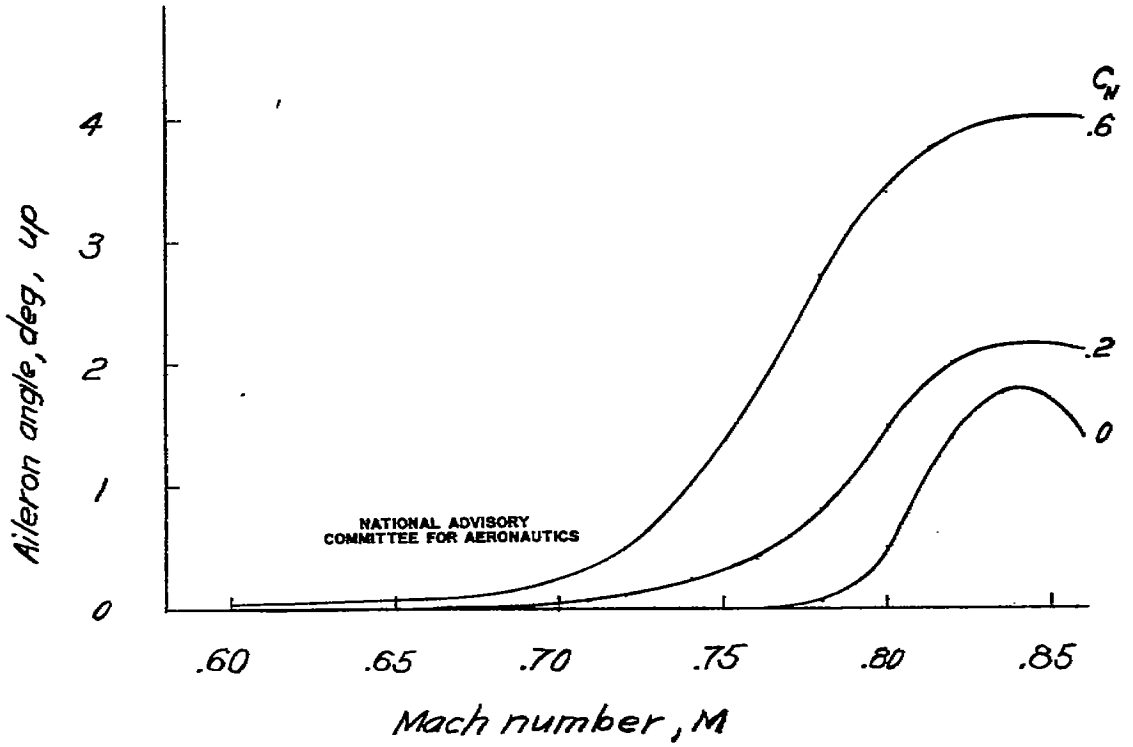

Figure 8.— Variation of aileron angle with Mach number for the test airplane.

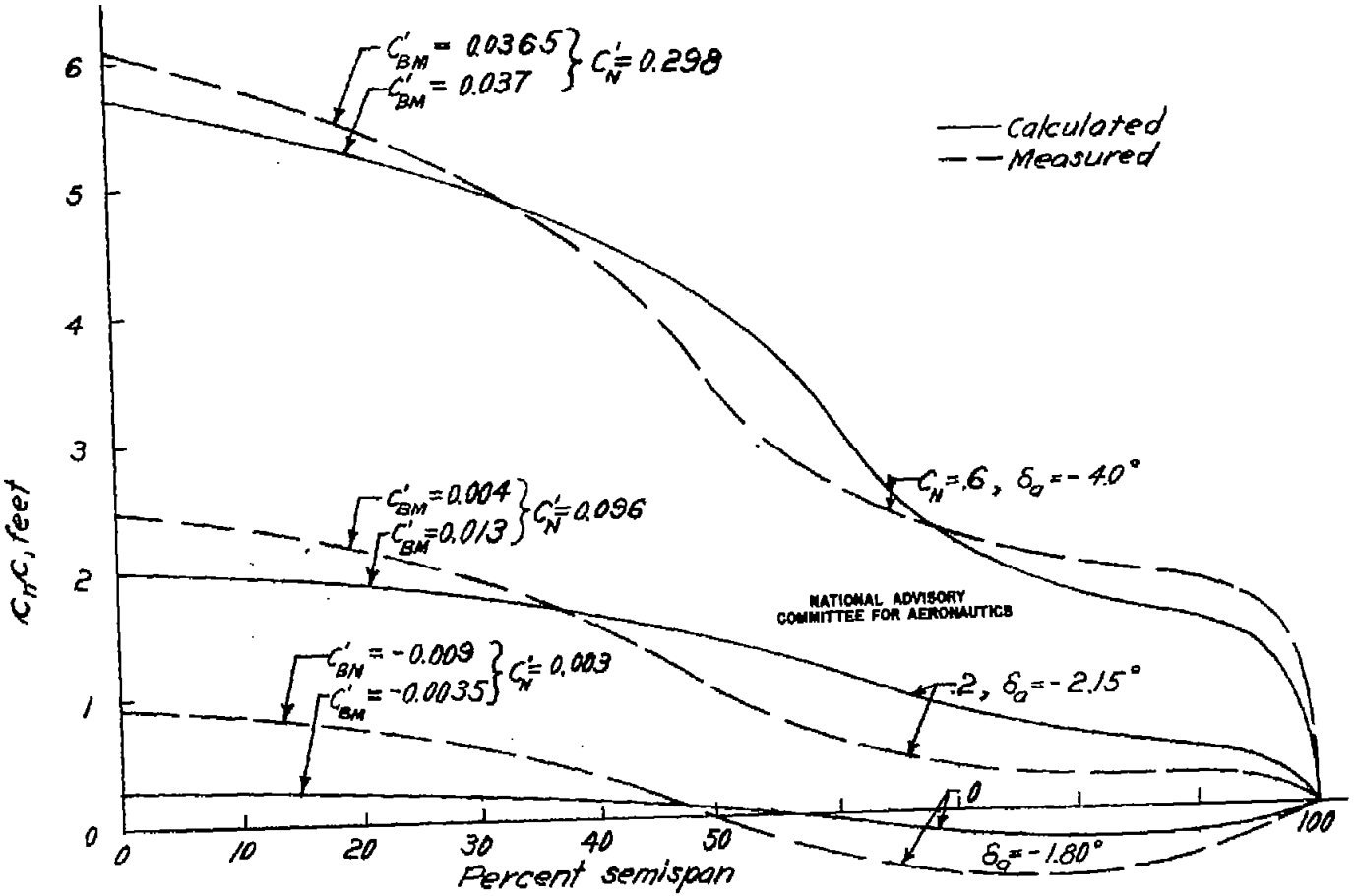

Figure 9.— Comparison between measured and calculated spanload distribution for Mach number of 0.84 using method of reference 2. Aileron deflected. (see fig. 7(c) for data with aileron undeflected.)

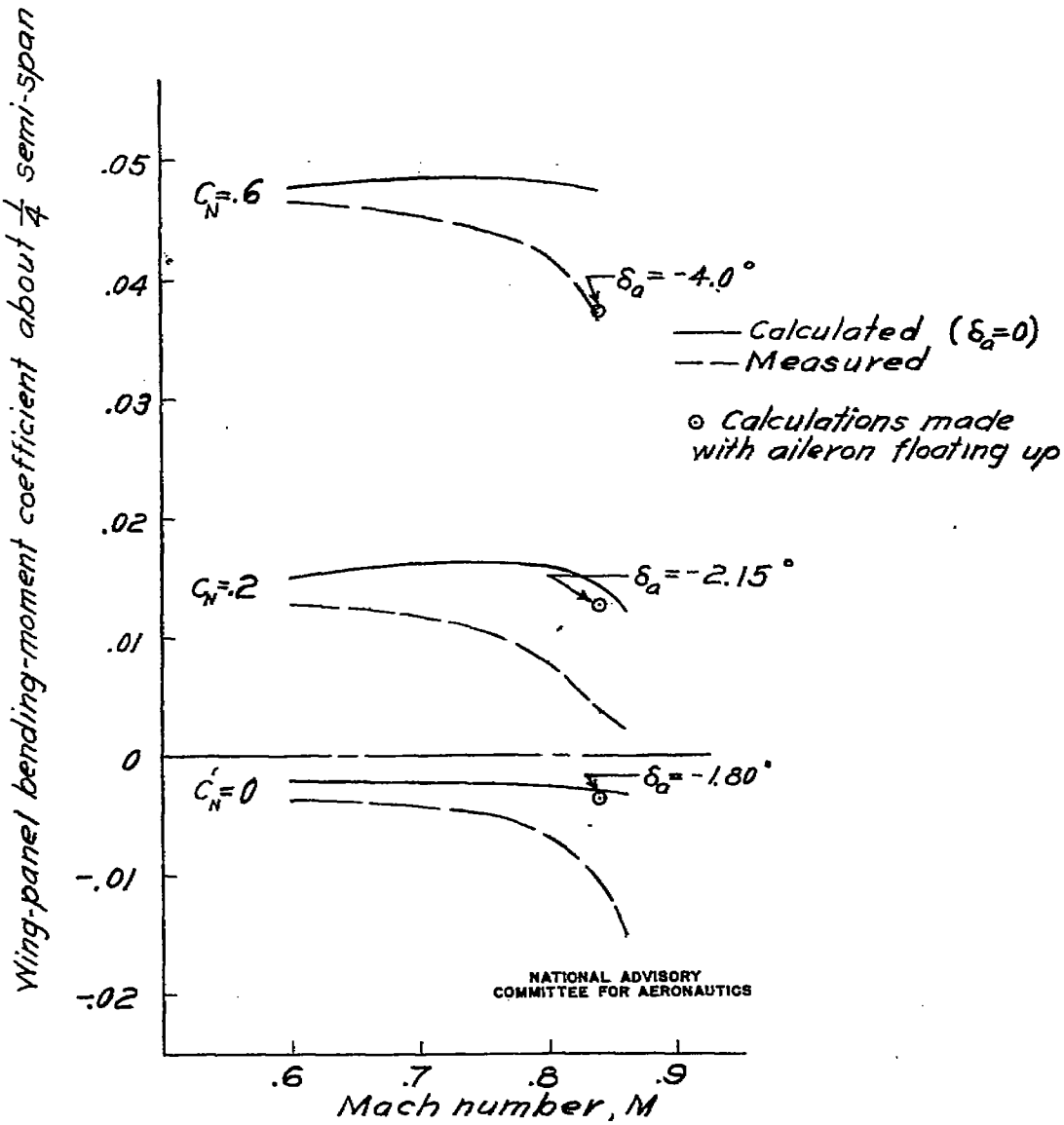

Figure 10.— Variation of wing-panel bending-moment coefficient about ¼ semispan with Mach number for the measured loading and the loading calculated by method of reference 2.

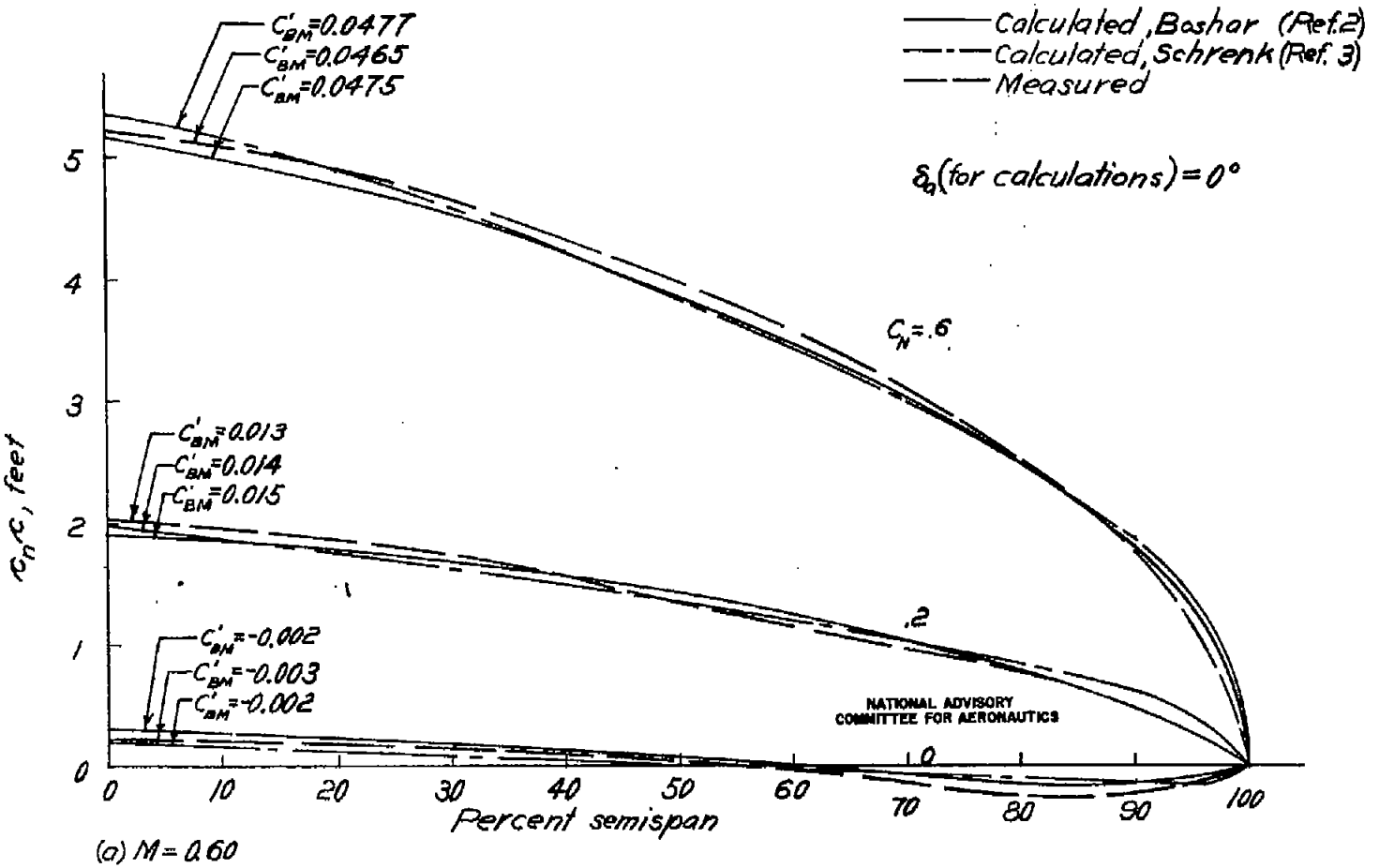

(a) M = 0.60

Figure 11.— Comparison between the spanload distributions calculated by the methods of references 2 and 3 and the results of flight tests.

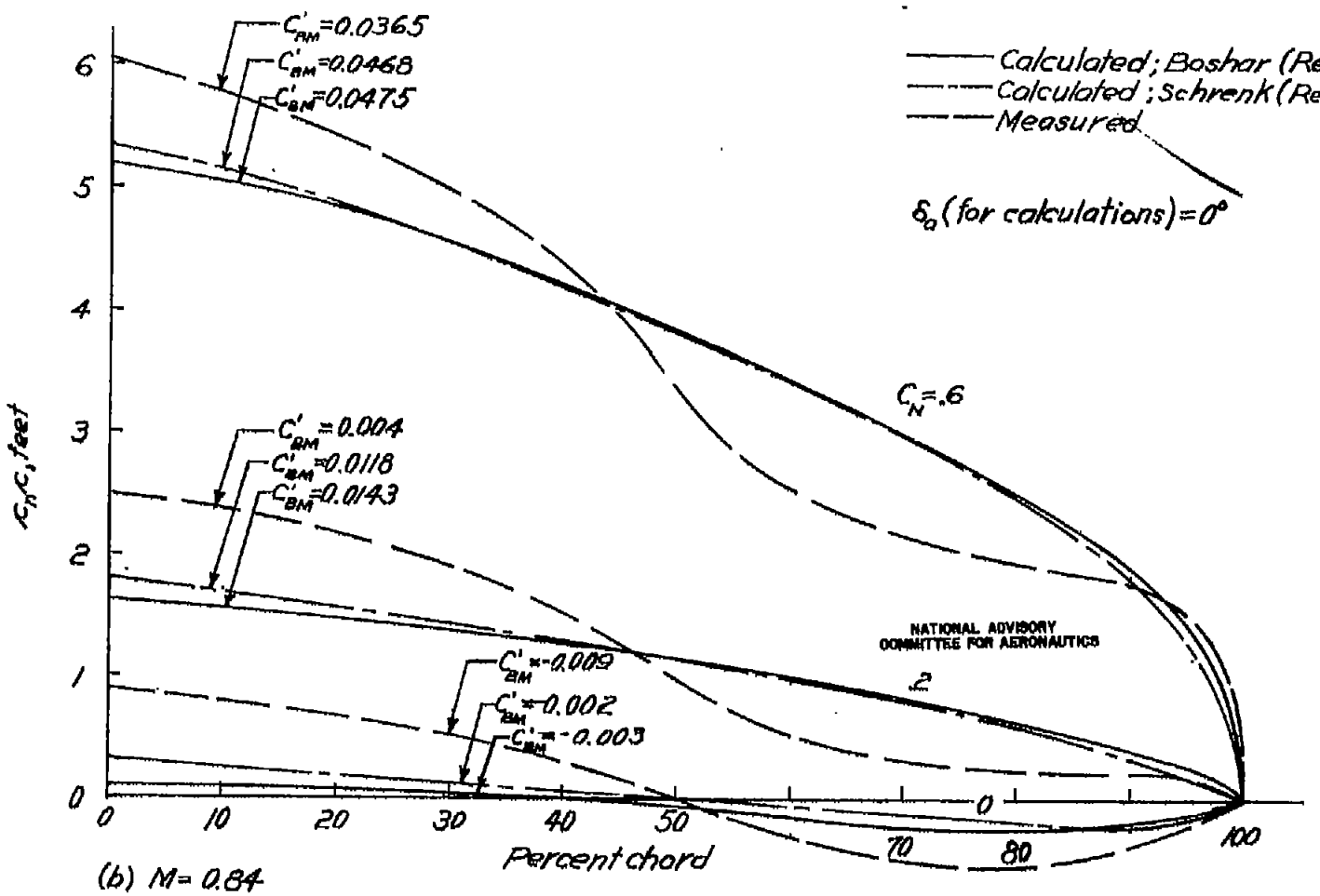

(b) M= 0.84

Figure 11.— Continued.

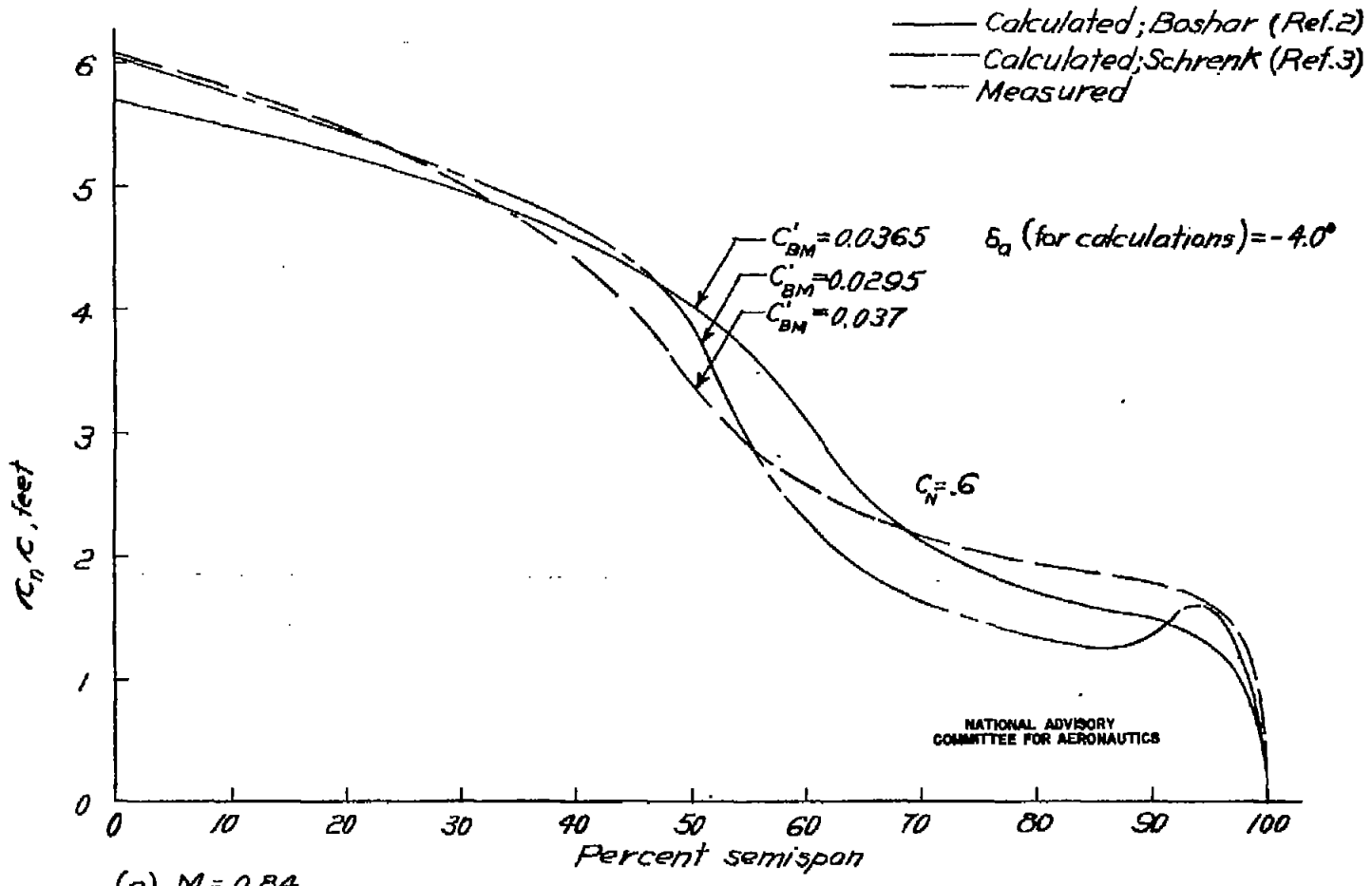

(c) M = 0.84

Figure 11.— Concluded.